

LARGE -GRAINED POLYCRYSTALLINE SILICON FILMS ON GLASS BY EPITAXIAL THICKENING OF SEED LAYERS PREPARED BY ALUMINIUM INDUCED CRYSTALLISATION

G Ekanayake [1], T Quinn [1], H Reehal [1], B Rau [2], S Gall [2]

[1] London South Bank University, 103 Borough Road, London, SE1 0AA, UK
Tel:+44 (0)20 7815 7513, Fax:+44 (0)20 7815 7699, E-mail: reehals@lsbu.ac.uk
[2] Hahn-Meitner-Institut Berlin, Kekuléstr. 5, D-12489, Berlin, Germany

ABSTRACT: This work reports on the improvement made during low temperature ($\leq 550^\circ\text{C}$) epitaxial growth of Si films on polycrystalline seed layers by adding argon to the deposition chamber during electron-cyclotron resonance chemical vapor deposition (ECRCVD) overgrowth. Seed layers with a preferred (100) orientation and grain sizes approaching $\sim 10\mu\text{m}$ were produced by aluminium-induced crystallization and layer exchange on glass. They were then chemically-mechanically polished before use. High quality epitaxial overgrowth has been achieved on these layers to a thickness of $2.7\mu\text{m}$ using argon in the ECR plasma. Without argon, the films are more defective and exhibit adverse structural changes at a smaller thickness compared to films grown with argon addition. The role of argon in the growth process is briefly discussed.

Keywords: Si-Films, Epitaxy, PECVD

1 INTRODUCTION

Polycrystalline silicon (poly-Si) films on glass show promise for cheap and efficient thin film solar cells but directly forming layers with sufficiently large grain size and thickness is challenging due to the amorphous nature and limited thermal stability of glass. A potential solution to this problem is to form thin, large grained poly-Si films by growth and subsequent crystallisation below the softening point of glass. These can then be used as templates for low temperature epitaxial thickening to produce absorber films [1,2]. Such seed layers have been fabricated by aluminium induced crystallisation (AIC) of amorphous silicon (a-Si) and, in particular, the aluminium-induced layer exchange (ALILE) process [3-5]. This produces silicon layers which are polycrystalline in nature with grains over $10\mu\text{m}$ in size and a preferred (100) orientation.

Epitaxial thickening of these layers has been reported at growth temperatures of $\sim 600^\circ\text{C}$ by electron-cyclotron resonance CVD (ECRCVD) [1] and ion-assisted deposition (IAD) [6]. In addition to large grain sizes it has been shown that a (100) preferential orientation of the seed layer is favourable for epitaxial thickening while smoothing and removal of surface oxide are also prerequisites for good epitaxial growth [1,3,6]. The use of these epitaxial layers as absorbers in simple solar cell structures has produced promising open circuit voltages of 400mV (ECRCVD) [7] and 440mV (IAD) [8].

In this work we report on the epitaxial thickening by ECRCVD of AIC poly-Si seed layers formed on glass. In particular, we present new results on the role that adding small amounts of Ar to the ECR discharge plays in improving the epitaxial film quality.

2 EXPERIMENTAL

2.1 Seed layer preparation

Seed layers were prepared at the Hahn-Meitner-Institut by ALILE. DC sputtering was used to deposit aluminium, followed by amorphous Si layers on Schott Borofloat33 glass. Between depositions the aluminium was exposed to atmosphere for 2h to allow oxide formation essential for large grain sizes after ALILE [3].

The layer exchange was performed by annealing at 500°C for 6h. This was followed by chemical-mechanical polishing (CMP).

2.2 ECRCVD Overgrowth

ECRCVD overgrowth was conducted at London South Bank University using a growth system described previously [9]. The cleaning procedure of seed-layer substrates consisted of ultrasonic cleaning with acetone (10min), etching in piranha solution (10min), rinsing in de-ionised water (8mins), dipping in 2% HF (30s), rinsing by de-ionised water and finally drying by nitrogen. Both during heating up to the deposition temperature and subsequent cooling, the substrate was subjected to a flow of 30 sccm of hydrogen at 6.0×10^{-3} mbar pressure.

The growth conditions, given in Table I, were optimised for epitaxial growth on single crystal, p+ boron-doped wafers. While hydrogen was introduced into the microwave plasma cavity, silane and argon, when used, was injected downstream of the cavity at the top of the growth chamber. No dopant gases were used. The resulting growth rate was $\sim 15\text{nm/min}$ for both deposition with and without argon.

Table I: Conditions for Si deposition on seed layers

Parameter	Value
H ₂ flow rate (sccm)	30
SiH ₄ flow rate (sccm)	2
Ar flow rate (sccm)	0 or 5
Total pressure (mbar)	6.0×10^{-3}
Microwave power (W)	500
Temperature ($^\circ\text{C}$)	500-550

2.3 Characterisation

Electron backscatter diffraction (EBSD) data was captured by an Oxford Instruments INCA system using a 20kV electron beam from a Hitachi S4300 FE SEM. TEM measurements on cross sections prepared using ion milling were carried out at CSMA-MATS (UK). Raman spectra were collected in a Renishaw 2000 system using the 488 nm line of an Ar ion laser. AFM measurements were performed using a Digital Instruments Multimode

scanning probe microscope while a Dektak 6m profilometer was used to measure film thicknesses. XRD measurements were performed in a Philips X'Pert MRD system by keeping the incident angle low (2.8°) to increase the film contribution and changing the detector angle (2θ).

3 RESULTS

3.1 Seed Layer Preparation

AFM images of the seed layer (Fig. 1) after CMP show remarkably smooth layers with average roughness (Ra) less than 0.5nm.

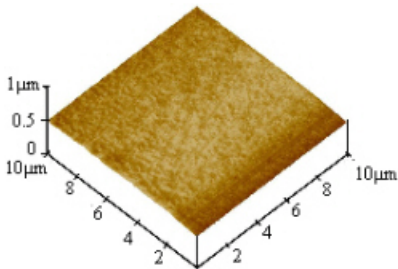


Figure 1: AFM of seed layer

The seed layer Si TO phonon Raman spectrum in Fig. 2 confirms that the silicon is unstressed and high quality crystalline on account of the peak position, 520.5 cm^{-1} , and full width at half maximum (FWHM), 5.6 cm^{-1} , being comparable to that expected for monocrystalline silicon.

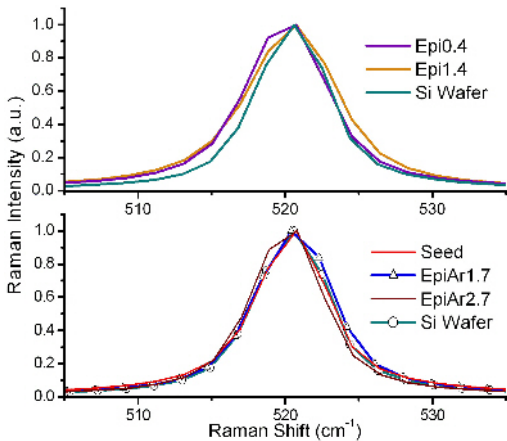


Figure 2: Si TO Raman peaks of a seed layer, overgrown samples and a reference Si wafer.

The EBSD orientation image map (OIM) (Fig. 3) confirms the crystalline quality of the ALILE process, showing a large proportion of grains over $5\mu\text{m}$ in size and with a preferred (100) orientation consistent with other ALILE Si samples [1,3].

3.2 ECRCVD Overgrowth

Raman spectra for samples Epi0.4, Epi1.4, EpiAr1.7 and EpiAr2.7 produced by ECR overgrowth on seed layers are shown in Fig. 2 (see Table II for details). While the peak position of all samples remains within 0.3 cm^{-1} of that expected of crystalline silicon, suggesting that there is little stress in the film, the FWHM of the

samples deposited without argon are larger, with the thicker sample (Epi1.4) especially wide. The results are consistent with a general trend of increasing FWHM with thickness seen in similar samples deposited without argon. This suggests that the microstructure of such low temperature epitaxy becomes increasingly defective with thickness, a result found by others [10]. Samples grown on monocrystalline silicon under the same growth conditions without Ar do not show a significant variation in FWHM with thickness ($\sim 5.7\text{-}6.0\text{ cm}^{-1}$) but do show an increasing level of stress as judged by the shift of the peak towards higher wavenumbers (by $+1.4\text{ cm}^{-1}$ for a thickness of $1.4\text{ }\mu\text{m}$).

Interestingly, both samples overgrown with argon added to the deposition gas show an invariance of the Raman FWHM with thickness, with even the thicker layer (EpiAr2.7) having a FWHM comparable to that of a silicon wafer. This suggests a high crystalline quality.

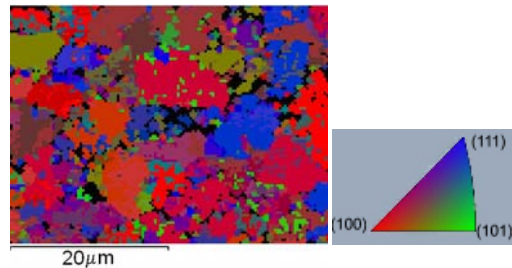


Figure 3: EBSD OIM in the sample normal direction of a seed layer with corresponding colour key showing the grain orientations.

Table II: Data for epitaxially overgrown samples

Sample	Ar flow (sccm)	Thickness (μm)	Area used by grains with size $>5\mu\text{m}$ (%)	FWHM of Si Raman Peak (cm^{-1})
Epi0.4	0	0.4	30	6.1
Epi1.4	0	1.4	8	6.9
EpiAr1.7	5	1.7	51	5.4
EpiAr2.7	5	2.7	7	5.3

Fig. 4 shows EBSD OIMs and inverse pole figures in the sample normal direction for samples EpiAr1.7 and EpiAr2.7. The OIMs of Epi0.4 and Epi1.4 are not shown but were similar to EpiAr1.7 and EpiAr2.7, respectively. The similarity between the EBSD maps of sample EpiAr1.7 (and Epi0.4) and the seed layer (Fig. 3) is striking. Coupled with the Raman results, this is a good indicator of epitaxial growth. As an indicator of grain size, Table II lists the area of each sample occupied by grains with a size $>5\mu\text{m}$. The thicker samples deposited with and without argon, EpiAr2.7 and Epi1.4, show smaller grain sizes and a more random orientation. These results are particularly interesting as Epi1.4 is slightly thinner than EpiAr1.7 and EpiAr2.7 had a small Raman FWHM. In large grain poly-Si the latter suggests a lower density of intra-grain defects but eventually there is a loss of grain size and orientation with thickness as in the case of films grown without argon. This loss, however, occurs at a higher thickness where argon was used. These results give further proof to the beneficial effect of argon addition during growth.

The difference in orientation between the samples grown with and without Ar is illustrated by Fig. 5. This

plots the proportion of film area lying within an angular range, α , of the (001) direction obtained from the EBSD maps. The data shows that samples EpiAr1.7 and Epi0.4 have a similar orientation with a stronger (100) character compared to samples EpiAr2.7 and Epi1.4 whose behaviour is also very similar to each other.

Due to the relative difficulty of epitaxially growing silicon at low temperatures on substrates with an orientation differing from (100), it might be expected that such grains in the seed layers would lead to a loss of epitaxy for the thicker overgrowths [3]. In spite of this, distinct silicon Kikuchi line patterns could be observed for over 95% of the film area in even the thickest samples, immediately showing that crystalline growth has occurred in nearly all the film area.

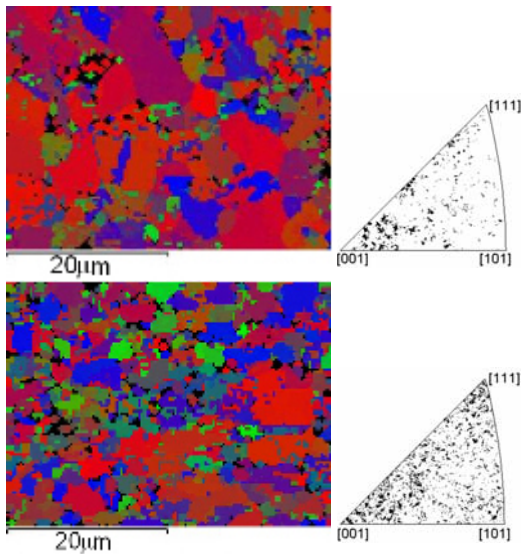


Figure 4: OIMs and inverse pole figures of EpiAr1.7 (top) and EpiAr2.7 (bottom).

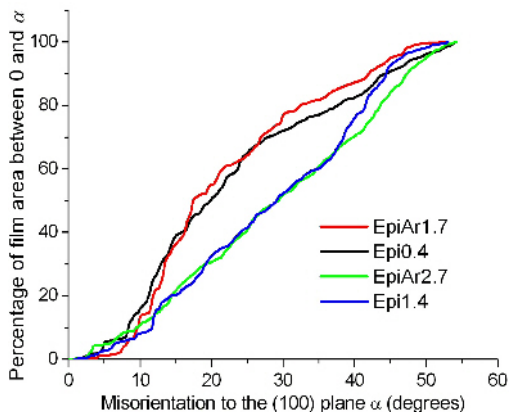


Figure 5: Proportion of film area within an angular range, α , of the (100) orientation determined from EBSD OIMs. A steeper gradient at low angles suggests a stronger preferred orientation.

Direct proof of epitaxy is further provided by cross-sectional TEM images of Epi1.4 and EpiAr1.7 (Fig. 6). These show a continuation of the seed layer structure into the overgrown film and also a relatively low concentration of defects in EpiAr1.7. Sample Epi1.4, however, shows a more defective structure immediately after the interface between the seed layer and ECRCVD

growth. The difference between the samples shows yet further evidence of the positive effect of argon addition during growth.

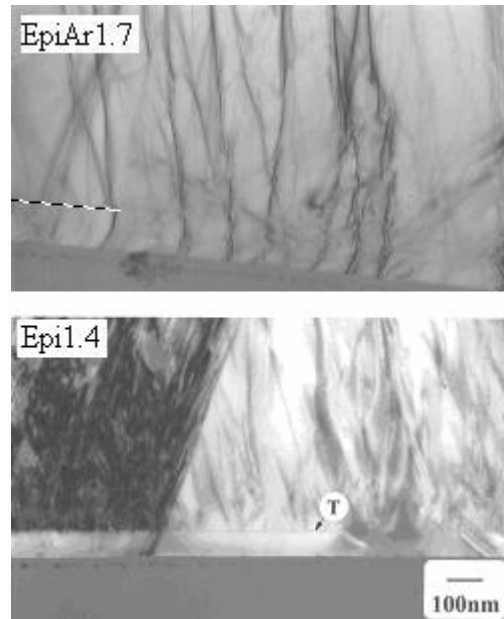


Figure 6: TEM images of EpiAr1.7 and Epi1.4. Interface between seed layer and overgrowth is indicated by dotted line (top) and symbol “T” (bottom).

XRD graphs for samples Epi1.4 and EpiAr2.7 (Fig 7) show sharp peaks confirming large grain size and no amorphous content. The peak heights have been normalised to the (111) reflection. There is a remarkable correlation between the two XRD graphs suggesting that the samples share a similar orientation, in agreement with the EBSD data of Fig. 5. Interestingly, both samples show an intense (311) peak which suggests a preferred (100) orientation in our XRD geometry when an incident angle of 2.8° is used. For comparison, a standard randomly orientated sample using a similar geometry shows a ratio of (311) to (111) peak intensities of $\sim 1/4$. Factors which need to be considered to account for differences between results from EBSD and XRD include the low ($\sim 1^\circ$) acceptance angle of misorientation of planes in XRD. Also while the whole sample (cm dimensions) is detected by XRD, much smaller areas are analysed by EBSD.

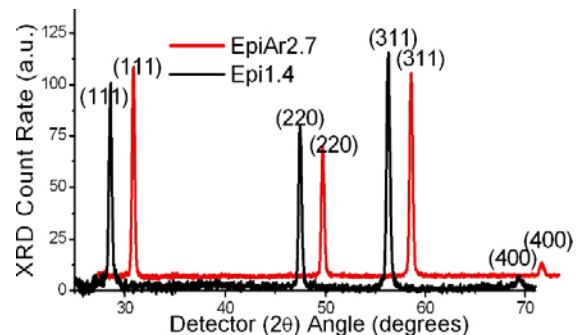


Figure 7: XRD data of samples Epi1.4 and EpiAr2.7 (EpiAr2.7 offset in x and y to prevent overlap)

AFM maps of samples Epi1.4 and EpiAr1.7 (Fig 8) illustrate the type of surface morphologies observed. In

general, with Ar addition the feature sizes are larger and more homogeneous. Faceting appears to be present. Shin et al. have suggested that twinning can lead to faceted surfaces during poly-Si film growth due to the evolution of rhombic pyramidal crystallites [11]. The variable surface of sample Epi1.4 probably reflects different orientation underlying grains. The trench-like features appear to occur at boundaries between different grains.

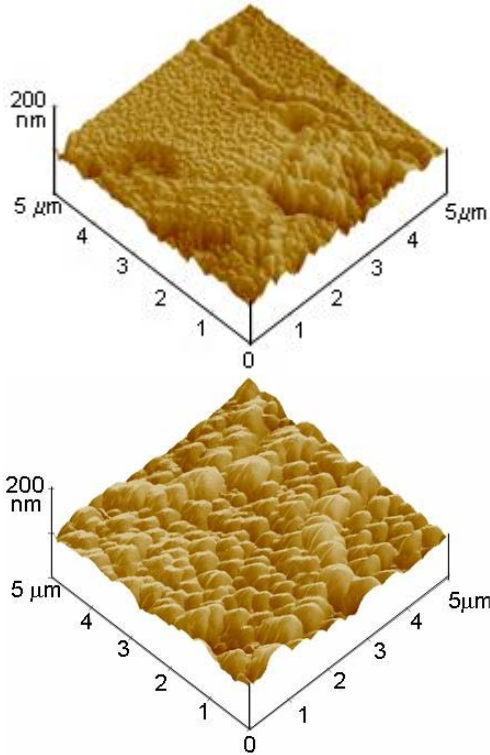


Figure 8: AFM maps of Epi1.4 (top) and EpiAr1.7 (bottom)

Finally, some preliminary electrical characterisation of the layers deposited using Ar has been carried out. The films are n-type with a conductivity activation energy of ~ 0.08 eV. Four point probe measurements give a figure of $\sim 2\text{-}3$ Ω cm for the room temperature resistivity.

4 DISCUSSION

The beneficial role of introducing argon gas into the ECRCVD chamber during overgrowth requires some explanation. It is likely that argon affects the density and energy of ions in the chamber. In an ECRCVD plasma, energetic ions may donate energy to the surface species increasing their mobility and removing loosely bound species, resulting in improved films. This must be balanced by damage that can also occur by energetic bombardment. Indeed, it is known that there is an optimum energy (~ 20 eV) in low temperature epitaxial Si growth by ion beam deposition [12] and deviating from this value results in an increase of defects.

In this work the substrate electrode was left floating and monitoring the substrate bias showed that the bias changed from ~ -8 V in the absence of Ar to ~ -12 V when Ar was added to the chamber gas flow. The increasingly negative potential may suggest an increase

in energy of positive ions impinging on the surface but to confirm this, the value of plasma potential would also need to be measured. It is possible that as for ion beam deposition, there is an optimum ion energy for ECRCVD and the addition of argon brings the ions closer to this value. Interestingly, the addition of argon under the growth conditions used did not strongly affect deposition rate and it may be possible that the change in ion energy is offset by the change in ion density but more work needs to be done to confirm this.

5 SUMMARY

The epitaxial growth of silicon films up to ~ 2.7 μm thick has been achieved by ECRCVD at temperatures of ≤ 550 $^{\circ}\text{C}$ on poly-Si seed layers prepared by the ALILE process. EBSD orientation maps show $> 95\%$ of the film surface can be indexed suggesting large grained crystal growth has occurred on all grain orientations present in the seed layer. The addition of Ar to the hydrogen rich silane growth environment has been found to play an important role in determining the structural quality of the deposited films.

6 ACKNOWLEDGEMENTS

We would like to thank EPSRC and BP Solar for support and M Muske for seed layer preparation.

REFERENCES

- [1] B. Rau, J. Klien, J. Schneider, E. Conrad, I. Sieber, M. Stöger-Pollach, P. Schattschneider, S. Gall, W. Fuhs, Proc. 20th European PV Solar Energy Conf., Barcelona, 2005, p.1067.
- [2] A. G. Aberle, J. Crystal Growth, 287 (2006) 386.
- [3] S. Gall, J. Schneider, J. Klien, K. Hübener, M. Muske, B. Rau, E. Conrad, I. Sieber, K. Petter, K. Lips, M. Stöger-Pollach, P. Schattschneider, W. Fuhs, Thin Solid Films 511-512 (2006) 7.
- [4] P.I. Widenborg, A.G. Aberle, J. Crystal Growth 242 (2002) 270.
- [5] G. Ekanayake, T. Quinn, H.S. Reehal, J. Crystal Growth, 293 (2006) 351.
- [6] A. Straub, D. Inns, M.L. Terry, Y. Huang, P.I. Widenborg, A.G. Aberle, J. Crystal Growth, 280 (2005) 385.
- [7] B. Rau, J. Schneider, E. Conrad, S. Gall, Mater. Res. Soc. Symp. Proc. Vol. 910 (2006) A25.03.
- [8] A. Aberle, Proceedings of the 4th World Conference on Photovoltaic Energy Conversion, Waikoloa, 2006, in press.
- [9] S. Summers, H.S. Reehal, G.H. Shirkoohi, J. Appl. Phys. D: Appl Phys, 34 (2001) 1.
- [10] W.J. Varhue, J.L. Rogers, P.S. Andry, E. Adams, Appl. Phys. Lett., 68 (1996) 349.
- [11] S-D. Shin, D-W. Kim, D-I. Kim, D-Y. Kim, J. Crystal Growth, 274 (2005) 347.
- [12] J.W. Rabalais, A.H. Al-Bayati, K.L. Boyd, D. Marton, J. Kulik, Z. Zhang, W.K. Chu, Phys. Rev. B, 53 (1996) 10781.